WARSAW UNIVERSITY OF TECHNOLOGY Index 351733
FACULTY OF CIVIL ENGINEERING
COMMITTEE FOR CIVIL AND WATER ENGINEERING
POLISH ACADEMY OF SCIENCES ISSN 1230-2945

DOI: 10.24425/ace.2025.154138

ARCHIVES OF CIVIL ENGINEERING

Vol. LXXI ISSUE 2 2025

pp. 575–590

© 2025. Małgorzata Jarosińska, Tomasz Wróblewski.

This is an open-access article distributed under the terms of the Creative Commons Attribution-NonCommercial-NoDerivatives License (CC BY-NC-ND 4.0, https://creativecommons.org/licenses/by-nc-nd/4.0/), which permits use, distribution, and reproduction in any medium, provided that the Article is properly cited, the use is non-commercial, and no modifications or adaptations are made.

Research paper

Identification of damage to a steel I-beam based on changes in frequency and curvature of the mode shape in a steel-concrete composite beam

Małgorzata Jarosińska[1], Tomasz Wróblewski[2]

Abstract: This paper presents changes in modal parameters, i.e. natural frequencies and the curvature of the mode shape, as a result of damage in the steel I-beam of a composite member. A steel-concrete composite beam was analyzed, for which numerical simulations (rigid finite element model) and experimental tests were carried out. The damage analyzed was intended to simulate actual propagation of cracking in the steel I-beam. Two levels of damage occurring at two different locations in the beam were studied. The value of frequency changes of experimental and numerical evaluations have shown high consistency (margin of a few percent). Natural frequencies turned out to be sensitive to the introduced damage – their values decreased as the degree of damage in the beam increased. The Curvature Damage Factor was used to analyze the curvature of the mode of vibration. The results obtained in the numerical evaluations were satisfactory. In relation to experimental tests, lower effectiveness was achieved, which was most likely caused by a different density of the measurement grid compared to numerical analyses.

Keywords: damage diagnosis, mode shape curvature, natural frequencies, steel-concrete composite beams

[1]PhD., Eng., West Pomeranian University of Technology in Szczecin, Faculty of Civil and Environmental Engineering, al. Piastów 50a, 70-311 Szczecin, Poland, e-mail: jarosinska@zut.edu.pl, ORCID: 0000-0001-8427-0128
[2]Prof. ZUT, PhD., Eng., West Pomeranian University of Technology in Szczecin, Faculty of Civil and Environmental Engineering, al. Piastów 50a, 70-311 Szczecin, Poland, e-mail: wroblewski@zut.edu.pl, ORCID: 0000-0003-3731-1542

www.czasopisma.pan.pl PAN POLSKA AKADEMIA NAUK www.journals.pan.pl

1. Introduction

Steel-concrete composite beams are structural members where those materials are fastened by, a suitable connectors. Making use of mechanical properties of both materials, where steel operates in tension and concrete in compression, has made those types of members increasingly popular as an economical way of constructing buildings and bridges. The most important aspect of using composite members in structures is the safety. For complex engineering structures such as bridges, it is fairly common to use the structural health monitoring (SHM) systems [1–4]. The systems operate in a continuous manner. The goal of such monitoring is to detect hazards as soon as possible in order to ensure the highest safety for users. For structures susceptible to dynamic impacts, the SHM systems are based on the modal analysis. Damage occurring in the structure causes a disruption in the structure's operation, which changes its dynamic characteristics. This is reflected in the modal parameters of the system. Methods based on the analysis of changes in those parameters can be an effective tool in damage evaluation. Scientists around the world have been searching for decades for a method that would be fully effective in identifying damage to structures – both detecting and localizing it. An overview of methods for detecting damage by changing its dynamic properties can be found in [5–12].

One of the most commonly evaluated modal parameter for the identification of damages is the natural frequency. At the moment of structural disturbance (i.e. damage to the structure), the stiffness of the system changes, which is directly related to the reduction of the natural frequency. Analyses of vibration frequency changes in relation to damage in steel-concrete composite beams can be found in [13–16]. Above mentioned studies present analytical models and experimental evaluations of steel-concrete composite beams with different degrees of connection in the joint plane. The studies assessed different levels of damage occurring in the joints plane of the beams. Results have shown that axial vibration frequencies are insensitive to the damage introduced. On contrary, flexural vibration frequencies have shown elevated sensitivity, meaning they can be an important indicator in the diagnostic analysis of composite beams.

The second modal parameter that is often studied for evaluation of damages is the mode of natural frequency. Damage occurring in a system causes a local change in its mode of vibration, which can be used to localize it. For minor damage, analysis of only the shape of mode of vibration can sometimes be insufficient. Analysis of changes in the curvature of the mode shape has been proven effective. Pandey et al. [17] were first to use it as a tool for damage identification. Based on numerical tests performed for two beams, they have proved that the damage causes changes in the curvature of the mode shape. If the modes of vibration before and after the occurrence of damage are known, the curvature of mode shape can be determined for each measurement point as its second derivative, according to the relation [17]:

$$MC_p = \frac{\left(y_{p+1} - 2y_p + y_{p-1}\right)}{h^2} \tag{1.1}$$

where y_p is the component of the mode of vibration at point p, h – is the distance between neighbouring measurement points.

However, studying the curvature for each mode separately can be time-consuming. Analysis of the problem can become easier and faster using an parameter that takes into account more

than one mode of vibration. In their work [18] Wahab and De Roeck proposed the Curvature Damage Factor (CDF), a parameter which takes into account curvature changes for several modes of vibration simultaneously. The CDF parameter is determined by the Formula (1):

$$\text{CDF}_p = \frac{1}{N}\sum_{n=1}^{N}\left|\text{MC}_{p,n} - \text{MC}_{p,u}\right| \tag{1.2}$$

where: N – number of modes in the analysis, $\text{MC}_{p,n/p,u}$ – curvature of mode shape at point p for intact/damage state.

Analyses of changes in the mode of vibration caused by damage in composite structures can be found in [19]. Results are presented for numerical model and lab-tested steel-concrete composite beam, and two levels of damage. Global (using Modal Assurance Criterion MAC) and local (using Partial Modal Assurance Criterion PMAC) mode of vibration have been analysed. Changes in the curvature of mode shape were presented using CDF, which proved to be a good tool in localizing damage in composite beams.

Several studies can be found that present the attempt to find a fully effective method for identification of damage to various types of structures. With regard to steel-concrete composite beams, different approaches have been proposed in modal analysis that utilized a.o. Wavelet Transform (WT) [20], Modal Strain Energy (MSE) [21], Energy Transfer Ratio (ETR) [22–24], Convolutional Neural Networks (CNNs) [25].

The purpose of this study was to evaluate the feasibility of using methods based on modal analysis to identify damage to steel-concrete composite beams. This type of beams are often used as the main load-bearing girders in bridges, for which the aspect of safety is crucial. A numerical model as well as experimental tests have been prepared for studied beam. The damage was inflicted to the steel I-beam. Initially, a crack in the bottom flange has been made, which, with the increase of load, propagated further causing failure. Two different locations of crack has been studied. Identification of the resulting damage was carried out in two stages: 1) the changes in the natural frequency were observed to detect the occurrence of damage, 2) the changes in the curvature of mode shape were used to localize the damage.

2. Description of experimental research

The composite beam model consisted of an IPE 160 steel I-beam with a length of 3240 mm connected through a perfobond shear connector (10 mm thick and 45 mm wide) to a reinforced concrete slab 3200 mm long, 600 mm wide and 60 mm thick. The steel used in the study was S235JRG2, while the concrete was of C30/37 class. Fig. 1 and Fig. 2 present the schematics of the analyzed beam.

Experiments have been conducted for a free-free beam. The setup allows to ignore the effect of supports' susceptibility on the results. This simplifies the analysis of data. The beam was freely hanged on a set of steel lines. The lines were fixed to the nodes of the initial flexural mode of vibration for of a simply supported beam (Fig. 3).

Fifty-four points were marked on the beam (Fig. 4). Points labelled 1–52 were measurement points at which the responses were recorded using acceleration sensors. At points number

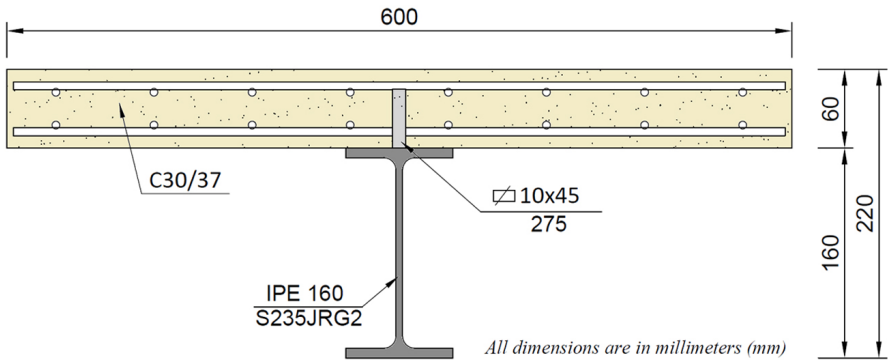

Fig. 1. Cross-section of the studied beam

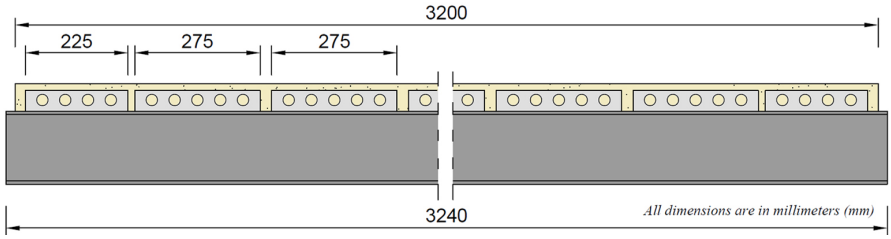

Fig. 2. Longitudinal section of the studied beam

Fig. 3. Experimental test stand and research apparatus

53 and 54 the modal hammer was used to excite vibration. With excitation at point 53 (in the $-Y$ direction), flexural vibrations of the beam were induced, while at point 54 (in the $+X$ direction) – axial vibrations. A multi-channel LMS SCADAS III signal analyzer connected to

a workstation equipped with LMS Test.Lab 13A software (LMS International) was used for the tests. Even though the measurements were taken at 52 points, in the following part of the work, only points located in the middle of the beam (2, 4, 6, 8, . . . , 52) were analyzed. This allowed the construction of a single-plane model of the beam.

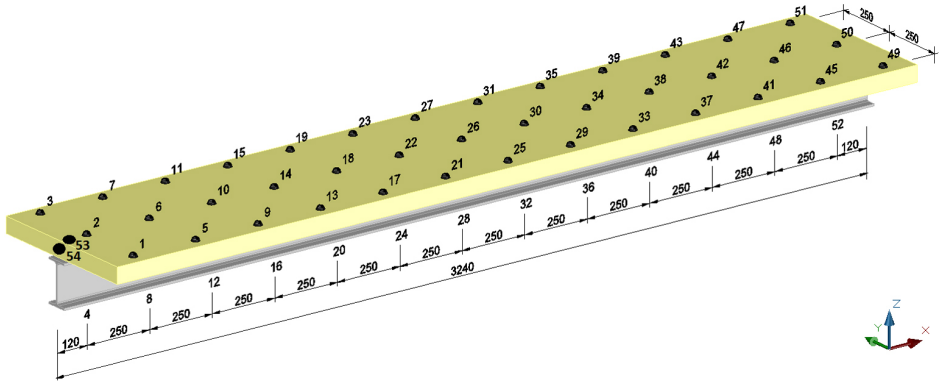

Fig. 4. Measurement and excitation points

The first five modes of flexural vibration and the first mode of axial vibration were determined for the points in the axial plane (2, 4, 6, 8, . . . , 52) (Table 1).

Table 1. Natural frequencies determined in the experimental tests

Flexural vibration					**Axial vibration**
$f_{\mathbf{1,exp}}$ [Hz]	$f_{\mathbf{2,exp}}$ [Hz]	$f_{\mathbf{3,exp}}$ [Hz]	$f_{\mathbf{4,exp}}$ [Hz]	$f_{\mathbf{5,exp}}$ [Hz]	$f_{\mathbf{1,exp}}$ [Hz]
75.06	178.90	287.98	389.31	489.70	579.66

Damage to the steel I-beam was performed by notching the bottom flange. Two notch depths were introduced: partial and full. The partial notch was made by cutting the flange on both sides of the web up to 50% of width. The full notch was made by cutting through the whole flange, reducing the operating cross-section by 100%. Figure 5 shows the damage (full notch) done to the bottom flange.

Damage was introduced at two locations shown as A and B in Fig. 6. Both points are located symmetrically with respect to the beam's axis, 1225 mm from the ends of the beam.

Four types of damage were introduced into the beam – U1, U2, U3, U4. In the first step, the flange at the location A was notched up to 50% (U1). Afterwards, the notch was extended through the whole length of the flange (U2). Similarly, in the next step, the damage was introduced at location B, with 50% notch depth (U3) and 100% notch depth (U4). Table 2 summarizes the analyzed damages U1–U4, and initial state U0.

Fig. 5. Damage to the bottom flange – full-depth notch

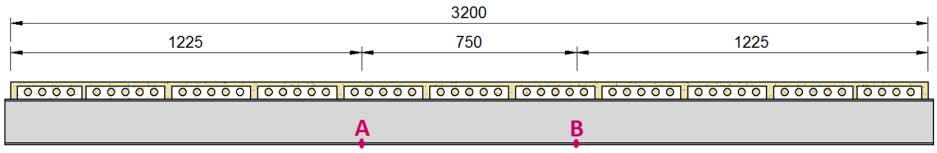

Fig. 6. Locations of the bottom flange damage points

Table 2. Types of damage in the I-beam

Beam condition		**U0**	**U1**	**U2**	**U3**	**U4**
Site of damage	A	–	50%	100%	100%	100%
	B	–	–	–	50%	100%

3. Beam model

The beam was modelled in a 2D plane using Rigid Finite Elements (RFEs) method [26]. In the first stage (so-called primary division), the model is divided into sections. In the second stage (so-called secondary division), a Spring-Damping Element (SDE) is placed in the center of each section, which reflects its elastic and damping properties. Neighbouring SDEs are connected by non-deformable RFEs. During the creation of the numerical model the steel and concrete components were treated separately. In addition, a change was made to the classical approach – for the steel part, a single SDE was replaced by a set of three SDEs located in the axes of the web and flanges. Thus, the elastic-damping properties of the entire section were distributed between the two flanges and the web. The introduced modification does not affect the obtained results, which was confirmed by the conducted tests. In turn, it allowed for an easier modelling of a local damage of the I-beam in the following stages of the work. The final beam model consisted of 66 RFEs, 33 for both steel I-beam and concrete slab (Fig. 7).

Beam's characteristics such as modulus of elasticity of steel (E_s = 210 GPa), Poissona coefficients (υ_s = 0.3; υ_c = 0.2), specific gravity (ρ_s = 7850 kg/m^3), were taken from available data. The density of the slab and cross-sections of concrete and steel were measured during the experiment. Missing characteristics determining the model's stiffness, e.g. Young's modulus E_c,

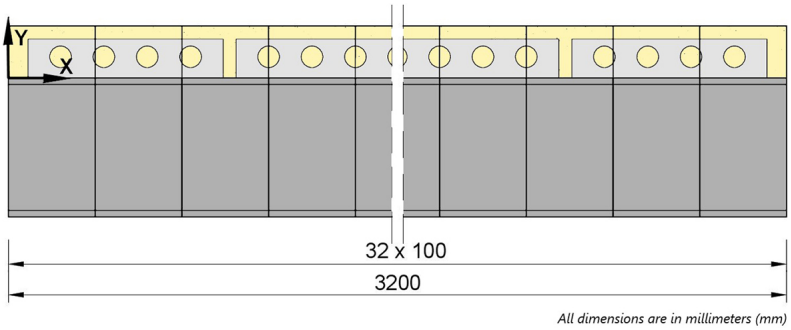

(a) primary division

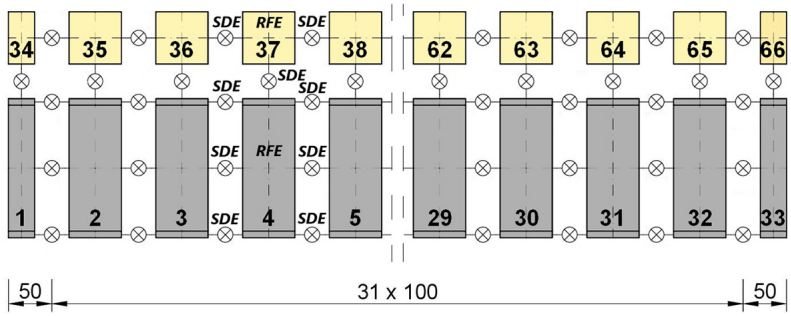

(b) secondary division

Fig. 7. RFE model of the beam; (a) primary division, (b) secondary division

that considers the reinforcement, and joint rigidity coefficients K_X, K_Y, were determined based of parametric identification. To do so, the MATLAB optimization package was used. The identification criteria were set as: 1) best fit of initial five flexural vibration frequencies, that were measured in experimental test and taken from numerical model, 2) complete fit of the initial axial vibration frequency determined for the numerical model and lab specimen. The latter criterion was chosen due to the high correlation of axial vibration to the E_c. It is important to highlight, that the coefficients K_X i K_Y reflect the stiffness of a single perfobond shear connector: K_X – tangent stiffness (X axis), K_Y – normal stiffness (Y axis). Results of conducted identification with the comparison of vibration frequencies is presented in Table 3.

As can be seen, a good fit of flexural vibration frequencies was obtained. The difference between the values from experimental tests and from numerical model did not exceed 1%. A good correlation of the axial frequencies was possible thanks to the adopted identification criterion. This mode of vibration was used only for the identification of the beam model and will no longer be used in further analyses.

The obtained value of elastic modulus of 28.7 GPa is lower than the value found in the Eurocode [27] for elastic modulus of concrete in relation to its compressive strength. However, the Standard does not take into account the type and size of aggregate. Lower value of the E_c modulus was a result of a smaller aggregate in concrete (up to 8 mm).

Table 3. Identification results of stiffness properties of the beam

$i \rightarrow$	1_{flex}	2_{flex}	3_{flex}	4_{flex}	5_{flex}	1_{axial}
$f_{i,\text{exp}}$ [Hz]	75.06	178.90	287.98	389.31	489.70	579.66
$f_{i,\text{num}}$ [Hz]	75.79	177.63	287.99	391.49	487.97	579.66
Δ_i	0.98%	0.71%	0.00%	0.56%	0.35%	0.00%
$\boldsymbol{E_c}$ [GPa]	28.7					
$\boldsymbol{K_X}$ [N/m]	8.10E+08					
$\boldsymbol{K_Y}$ [N/m]	2.78E+08					

In the following step, the comparison of modes of vibration obtained in numerical and experimental analysis was performed. For this purpose, MAC was used (Table 4). Due to the value of MAC coefficient for the fifth mode of vibration was only 0.47, it was decided not to include it in further analysis.

Table 4. Values of the MAC coefficient

Mode shape $\rightarrow$	1_{flex}	2_{flex}	3_{flex}	4_{flex}	5_{flex}
MAC	0.98	0.92	0.83	0.76	0.47

The numerical simulation of the damage to the bottom flange was then performed. The elastic properties of the corresponding SDEs modelling the bottom flange (A_f, $I_{z,f}$). has been modified. It was conducted to accommodate the reduction of the cross section due to notching of the flange (50% or 100% of length). Figure 8 shows the SDEs which were modified.

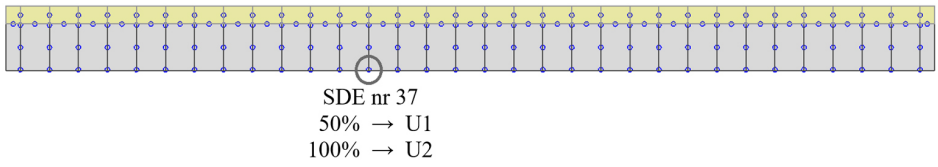

(a) U1/U2

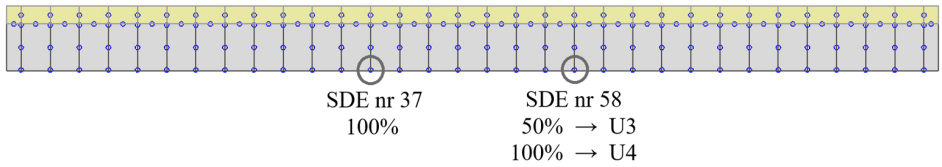

(b) U3/U4

Fig. 8. Damage to the model; a) U1/U2, b) U3/U4

4. Results

4.1. Natural frequencies

The effect of I-beam damage U1–U4 on the natural frequencies is shown below (Table 5, Table 6). Figure 9 presents the changes in frequencies obtained in the experimentally and numerical evaluations.

Table 5. Changes in the natural frequency as a result of inflicted damage – experimental test

Beam State →	**U0**	**U1**		**U2**		**U3**		**U4**	
$i \downarrow$	$f_{i,\mathrm{exp}}$ [Hz]	$f_{i,\mathrm{exp}}$ [Hz]	Δ_i [%]	$f_{i,\mathrm{exp}}$ [Hz]	Δ_i [%]	$f_{i,\mathrm{exp}}$ [Hz]	Δ_i [%]	$f_{i,\mathrm{exp}}$ [Hz]	Δ_i [%]
1	75.06	74.68	–0.51	72.09	–3.96	71.76	–4.40	70.24	–6.42
2	178.90	178.33	–0.32	175.17	–2.08	174.71	–2.34	172.62	–3.51
3	287.98	287.55	–0.15	286.58	–0.49	286.68	–0.45	286.35	–0.57
4	389.31	388.24	–0.27	384.30	–1.29	384.07	–1.35	382.04	–1.87

Table 6. Changes in the natural frequency as a result of inflicted damage – numerical model

Beam State →	**U0**	**U1**		**U2**		**U3**		**U4**	
$i \downarrow$	$f_{i,\mathrm{num}}$ [Hz]	$f_{i,\mathrm{num}}$ [Hz]	Δ_i [%]	$f_{i,\mathrm{num}}$ [Hz]	Δ_i [%]	$f_{i,\mathrm{num}}$ [Hz]	Δ_i [%]	$f_{i,\mathrm{num}}$ [Hz]	Δ_i [%]
1	75.79	74.95	–1.11	72.40	–4.47	71.68	–5.43	69.48	–8.33
2	177.63	176.75	–0.50	174.28	–1.89	173.25	–2.47	170.36	–4.09
3	287.99	287.89	–0.04	287.60	–0.13	287.51	–0.17	287.25	–0.25
4	391.49	390.50	–0.25	387.75	–0.95	386.72	–1.22	383.85	–1.95

As can be seen, the changes in the natural frequencies was similar in experimental and numerical evaluations. As was to be expected, an increase level of damage caused a decrease in the value of the vibration frequency, which is directly related to the loss of stiffness of the beam. The highest value of 8% was obtained in the numerical model for the first vibration frequency. The frequencies of the third mode of vibration remained almost intact with none of the changes exceeding 0.6%. Such small values of frequency changes are most likely due to the proximity of this mode of vibration nodes to the damage location.

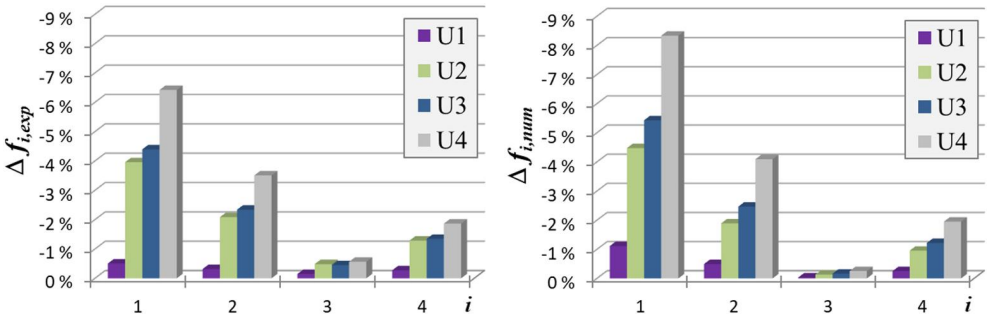

(a) Experimental test (b) Numerical model

Fig. 9. Changes in the natural frequency as a result of inflicted damage; (a) experimental test, (b) numerical model

4.2. Mode shape curvature

The curvature of the vibration mode shape was determined from relation (1.1). For the carried out analyses, only the displacement in the *Y* direction were considered, discarding the X direction. As the curvature of vibration was determined from mode shape (relations 1.1) the analysis ignored the outermost points of the beam – outermost RFEs in numerical analysis and outermost points in experimental tests. Based on the numerical simulations the initial check was performed to determine the changes in the curvature of mode shape due to the introduction of the damage. Figure 10 shows separately, for the steel and concrete parts the curvature of the mode shape for the undamaged state U0 and for one of the damage level – U2.

As shown in Fig. 10, the U2 damage caused a change in the curvature of the mode shape in the damage area. The changes were mostly visible in the steel part, which is a direct result of the damage to this element. However, not every mode was sensitive to the existing damage. Insignificant changes occurred for the third mode of vibration, which is due to the proximity of the curvature null mode.

The changes in the curvature were determined using CDF coefficient, which can take several modes simultaneously. The coefficient was determined for the modes of vibration for both steel and concrete parts. The insensitivity of the third mode of vibration to the damage done to the element, resulted in its exclusion from further analysis. The CDF coefficient was determined for the first, second and fourth mode of vibration as shown in Formula (1.2).

The curvature of the modes of vibration acquired in the experimental measurements was determined from the data. This means that the nodes in the modes of vibration coincide with the measurements points grid. Figure 11 presents the location of sensors along the beam's axis, and the location of damage.

Figure 12 and Fig. 13 present the results obtained for the damage levels U1 and U2 for numerical model and experimental tests, respectively. Figure 14 and Fig. 15 show the same results for the U3 and U4 damage levels. The node grid for the numerical model does not coincide with the grid of measurement points from the experimental setup.

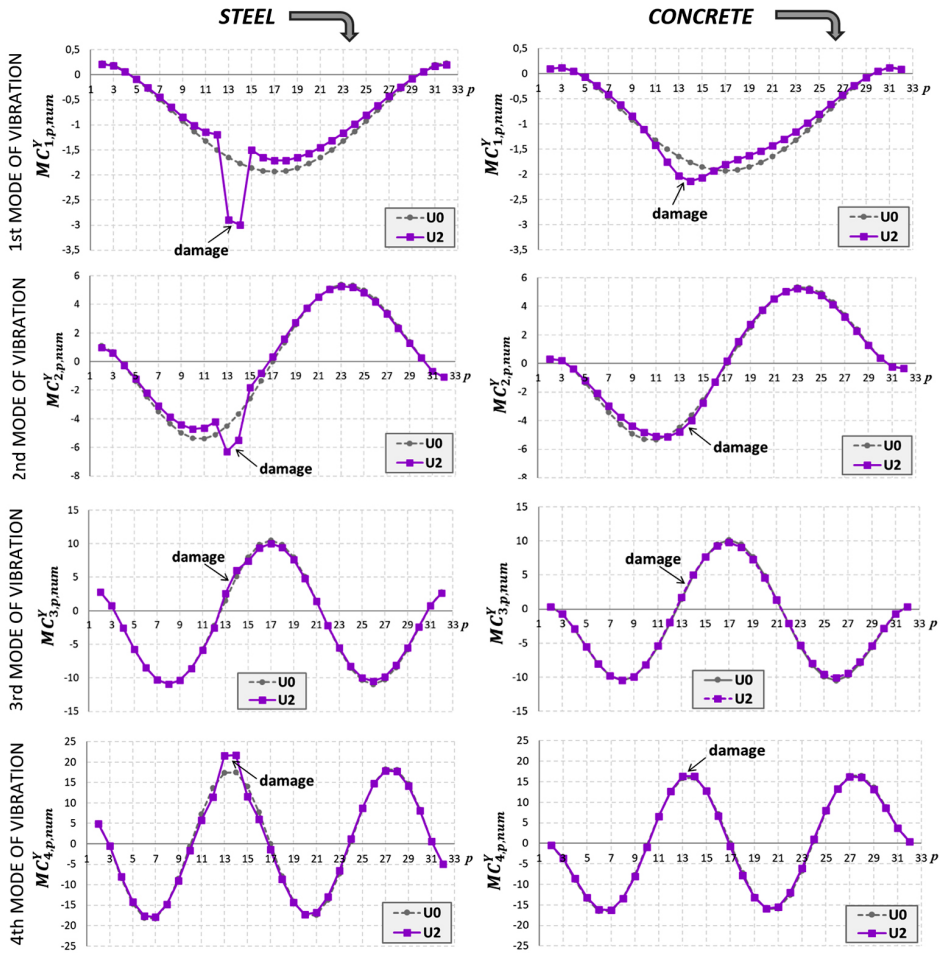

Fig. 10. Curvature of mode shape for the RFE model, U0 i U2 levels

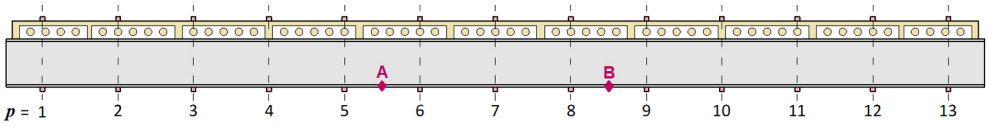

Fig. 11. Location of sensors along the beam, and damage points

Presented results have shown that the method of determining the location of damage based on the analysis of the curvature of vibration with the use of the CDF coefficient is effective. The numerical model allowed to easily pin point the location of introduced damage. In case of the experimental tests, for the U1 and U4 damage levels the highest values of the CDF coefficient were nearby the location of damage. However, for the U2 and U3 levels, the coefficient does

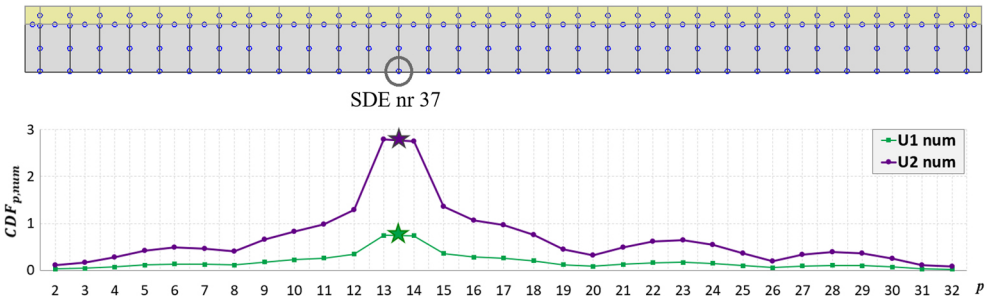

Fig. 12. The CDF for damage level U1, U2 in a model beam

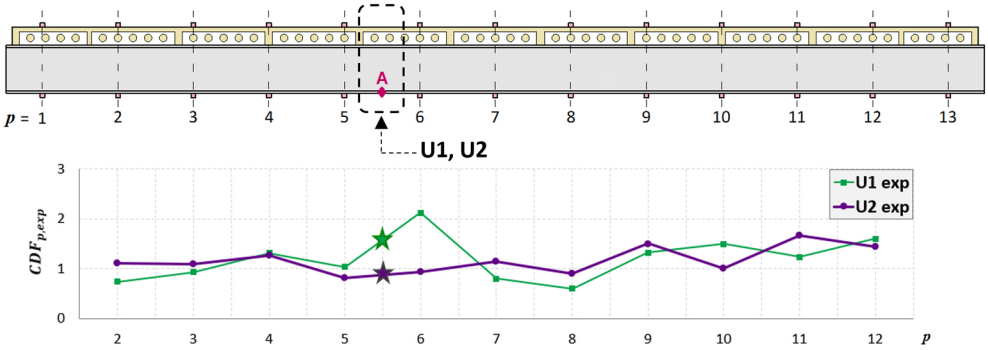

Fig. 13. The CDF for damage level U1, U2 in experimental tests

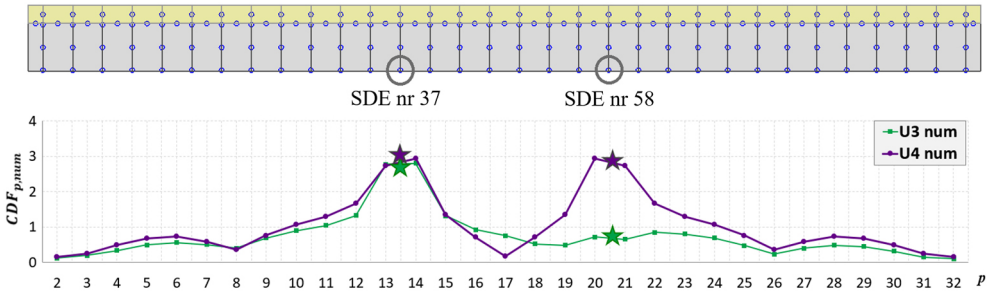

Fig. 14. The CDF for damage level U3, U4 in a model beam

not exhibit any distinctive values. It must be however highlighted, that the numerical model and real-life specimen had different grid density, with 31 nodes and 11 points, respectively. Therefore, it might be concluded that with higher density of measurement points on the real-life model, the location of introduced damage would be determined precisely.

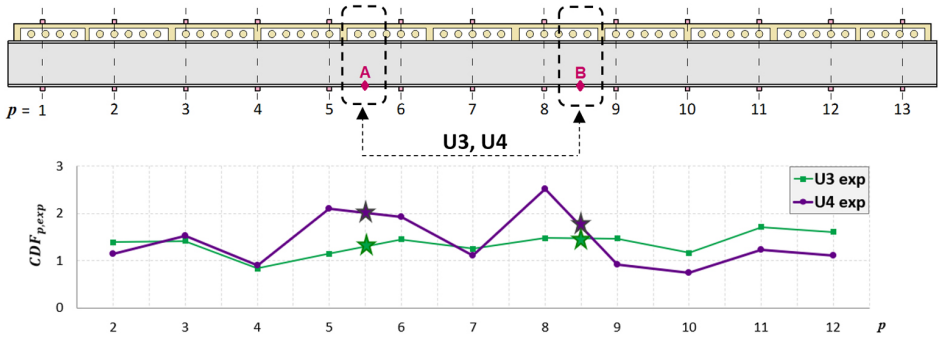

Fig. 15. The CDF for damage level U3, U4 in experimental tests

5. Summary

The study analysis the sensitivity of modal parameters to damage introduced to an I-beam in steal-concrete composite member. In the first part of the study the changes in natural frequencies were analysed to detect the damage. With the increase of the damage input, the natural frequency of the beam decrease, which was directly linked to its stiffness. A strong correlation of the change in frequency (reaching several percent) for both numerical model and experimental specimen was achieved. In the second part of the study the curvature of mode shape was evaluated, using the CDF coefficient, to determine the location of the damage. The evaluation of numerical model gave a satisfactory results. The change of the curvature allowed to determine the location of the damage on the bottom flange of the I-beam. The experimental results have shown satisfactory results in half of studied cases. The results can be considered as a good predictor of this method's applicability with moderate modifications. The accuracy of this method highly depends on the density of the measurements points grid. Therefore, it should be assumed that with the use of dense measurement grid, the effectiveness of this method would also be confirmed for experimental tests.

Performed analysis of the two-step identification of the damage to a composite beam was effective in determining the location of existing damage in numerical model. This confirm the high effectiveness of this method. The disadvantage of this method is however that it requires a sufficiently dense measurement grid. In case of monitoring a real-life structure, the limited number of possible sensors applied to the object can limit the reliable determination of modes of vibration, especially the higher ones. This can results in inability to determine the accurately the derivatives of consecutive modes of vibration. With improper density of measurement points, the curvature method can be burdened with an significant bias. More compacted grid can be achieved by using non-direct methods of measuring the vibration with laser doppler vibrometer. The effectiveness of this approach for complex structures can be found in [28].

Identification of damage to engineering objects is a complicated matter. The manuscript shows that even a significant damage can only cause small changes in the analyzed indicators. Currently, identifying damage based on a single measurements is difficult, but as shown, possible. However, attention should be given to non-stopping development of measurement

www.czasopisma.pan.pl PAN POLSKA AKADEMIA NAUK www.journals.pan.pl

techniques used in SHM. It is expected that in the next decades the development of measurement techniques will continue to grow exponentially, resulting in the increase of accuracy. New technologies enable more accurate measurements while reducing the cost. Lower cost of a SHM system allows new facilities to be equipped with a continuous monitoring. Thus, damage identification can be done not on the basis of a single measurements but only on the basis of statistical analysis of large sets of data. The method will eliminate the single measurement error and increase the accuracy.

References

[1] D. Balageas, "Introduction to Structural Health Monitoring", in *Structural Health Monitoring*. John Wiley & Sons, Ltd, 2006, pp. 13–43.

[2] H. Wenzel, *Health monitoring of bridges*. John Wiley & Sons, 2008.

[3] P.C. Chang, A. Flatau, and S.C. Liu, "Review Paper: Health Monitoring of Civil Infrastructure", *Structural Health Monitoring*, vol. 2, no. 3, pp. 257–267, 2003, doi:10.1177/1475921703036169.

[4] A.Z.O. Al-Hijazeen, M. Fawad, M. Gerges, K. Koris, and M. Salamak, "Implementation of digital twin and support vector machine in structural health monitoring of bridges", *Archives of Civil Engineering*, vol. 69, no. 3, pp. 31–47, 2023, doi:10.24425/ace.2023.146065.

[5] H. Sohn, C.R. Farrar, F. Hemez, and J. Czarnecki, "A Review ofmStructural Health Monitoring Literature 1996 – 2001", pp. 1–7, 2001.

[6] O. Avci, O. Abdeljaber, S. Kiranyaz, M. Hussein, M. Gabbouj, and D.J. Inman, "A review of vibration-based damage detection in civil structures: From traditional methods to Machine Learning and Deep Learning applications", *Mechanical Systems and Signal Processing*, vol. 147, art. no. 107077, 2021, doi:10.1016/j.ymssp.2020.107077.

[7] D. Montalvão, N.M.M. Maia, and A.M.R. Ribeiro, "A review of vibration-based structural health monitoring with special emphasis on composite materials", *Shock and Vibration Digest*, vol. 38, no. 4, pp. 295–324, 2006.

[8] S.W. Doebling, C.R. Farrar, and M.B. Prime, "A summary review of vibration-based damage identification methods", *Shock and Vibration Digest*, vol. 30, no. 2, pp. 91–105, 1998.

[9] S. Das, P. Saha, and S.K. Patro, "Vibration-based damage detection techniques used for health monitoring of structures: a review", *Journal of Civil Structural Health Monitoring*, vol. 6, no. 3, pp. 477–507, 2016, doi:10.1007/s13349-016-0168-5.

[10] R. Hou and Y. Xia, "Review on the new development of vibration-based damage identification for civil engineering structures: 2010–2019," *Journal of Sound and Vibration*, vol. 491, art. no. 115741, 2021, doi:10.1016/j.jsv.2020.115741.

[11] Y. Yang, Y. Zhang, and X. Tan, "Review on vibration-based structural health monitoring techniques and technical codes", *Symmetry*, vol. 13, no. 11, pp. 1–18, 2021, doi:10.3390/sym13111998.

[12] M. Rucka, "Special Issue: 'Non-Destructive Testing of Structures", *Materials*, vol. 13, no. 21, pp. 1–6, 2020, doi:10.3390/ma13214996.

[13] A. Morassi and L. Rocchetto, "A Damage Analysis of Steel-Concrete Composite Beams Via Dynamic Methods: Part I. Experimental Results", *Journal of Vibration and Control*, vol. 9, no. 5, pp. 507–527, 2003, doi:10.1177/1077546303009005002.

[14] M. Dilena and A. Morassi, "A Damage Analysis of Steel-Concrete Composite Beams Via Dynamic Methods: Part II. Analytical Models and Damage Detection", *Journal of Vibration and Control*, vol. 9, no. 5, pp. 529–565, 2003, doi:10.1177/1077546303009005003.

[15] M. Dilena and A. Morassi, "Vibrations of steel-concrete composite beams with partially degraded connection and applications to damage detection", *Journal of Sound and Vibration*, vol. 320, no. 1–2, pp. 101–124, 2009, doi:10.1016/j.jsv.2008.07.022.

[16] M. Dilena and A. Morassi, "Experimental modal analysis of steel concrete composite beams with partially damaged connection", *Journal of Vibration and Control,* vol. 10, no. 6, pp. 897–913, 2004, doi:10.1177/1077546304041370.

[17] A.K. Pandey, M. Biswas, and M. Samman, "Damage detection from changes in curvature mode shapes", *Journal of Sound and Vibration*, vol. 145, pp. 321–332, 1991.

[18] M.M.A. Wahab and G.D. Roeck, "Damage Detection In Bridges Using Modal Curvatures: Application To A Real Damage Scenario", *Journal of Sound and Vibration,* vol. 266, no. 2, pp. 217–235, 1999.

[19] M. Jarosińska and S. Berczyński, "Changes in frequency and mode shapes due to damage in steel–concrete composite beam", *Materials*, vol. 14, no. 21, pp. 1–18, 2021, doi:10.3390/ma14216232.

[20] M. Szumigała, A. Pełka-Sawenko, T. Wróblewski, and M. Abramowicz, "Damage Detection of Steel-Concrete Composite Beam", *Civil and Environmental Engineering Reports*, vol. 28, no. 3, pp. 30–49, 2018, doi:10.2478/ceer-2018-0033.

[21] F. Sadeghi, Y. Yu, X. Zhu, and J. Li, "Damage identification of steel-concrete composite beams based on modal strain energy changes through general regression neural network", *Engineering Structures*, vol. 244, art. no. 112824, 2021, doi:10.1016/j.engstruct.2021.112824.

[22] T. Wróblewski, M. Jarosińska, and S. Berczyński, "Application of ETR for diagnosis of damage in steel-concrete composite beams", *Journal of Theoretical and Applied Mechanics*, vol. 49, no. 1, pp. 51–70, 2011.

[23] T. Wróblewski, M. Jarosińska, M. Abramowicz, and S. Berczyński, "Experimental validation of the use of energy transfer ratio (ETR) for damage diagnosis of steel-concrete composite beams", *Journal of Theoretical and Applied Mechanics*, vol. 55, no. 1, pp. 241–252, 2017, doi:10.15632/jtam-pl.55.1.241.

[24] T. Wróblewski, M. Jarosińska, and S. Berczyński, "Damage location in steel-concrete composite beams using energy transfer ratio (ETR)", *Journal of Theoretical and Applied Mechanics*, vol. 51, no. 1, pp. 91–103, 2013.

[25] A. Bilotta, A. Morassi, and E. Turco, "Damage identification for steel-concrete composite beams through convolutional neural networks", *Journal of Vibration and Control*, vol. 30, no. 3-4, pp. 876-889, 2023, doi:10.1177/10775463231152926.

[26] J. Kruszewski, S. Sawiak, and E. Wittbrodt, *Metoda sztywnych elementów skończonych w dynamice konstrukcji (The rigid finite element method in dynamics of structures).* Wydawnictwa Naukowo-Techniczne, 1999.

[27] PN-EN 1992-1-1: 2008 Eurokod 2: Projektowanie konstrukcji z betonu. Część 1-1: Reguły ogólne i reguły dla budynków. PKN, 2008.

[28] E. Manoach, J. Warminski, L. Kloda, and A. Teter, "Numerical and experimental studies on vibration based methods for detection of damage in composite beams", *Composite Structures*, vol. 170, pp. 26–39, 2017, doi:10.1016/j.compstruct.2017.03.005.

Identyfikacja uszkodzeń dwuteownika stalowego na podstawie zmian częstotliwości oraz krzywizny postaci drgań w stalowo-betonowej belce zespolonej

Słowa kluczowe: diagnostyka uszkodzeń, krzywizna postaci drgań, częstotliwość drgań własnych, stalowo-betonowe belki zespolone

Streszczenie:

W pracy przedstawiono zmiany parametrów modalnych tj. częstotliwości drgań własnych oraz krzywizny postaci drgań w wyniku uszkodzeń powstałych w dwuteowniku stalowym belki zespolonej. Analizie poddano belkę zespoloną stalowo-betonową, dla której przeprowadzono symulacje numeryczne (w modelu RFE) oraz badania doświadczalne. Analizowane uszkodzenie miało symulować rzeczywiste postępujące pęknięcie dwuteownika stalowego. Badano dwa poziomy uszkodzeń pojawiające się w dwóch różnych miejscach belki. Uzyskano bardzo wysoką zgodność zmian częstotliwości (na poziomie kilku procent) określonych na podstawie numerycznej i eksperymentalnej symulacji uszkodzeń. Częstotliwości drgań okazały się być wrażliwe na wprowadzone uszkodzenia – ich wartości obniżały się wraz ze wzrostem stopnia uszkodzeń w belce. Do analizy krzywizny postaci drgań wykorzystano parametr CDF.

www.czasopisma.pan.pl PAN POLSKA AKADEMIA NAUK www.journals.pan.pl

W tym zakresie otrzymano zadowalające wyniki na podstawie przeprowadzonych analiz numerycznych. W odniesieniu do badań eksperymentalnych uzyskano mniejszą skuteczność, co najprawdopodobniej spowodowane było zróżnicowaną gęstością siatki pomiarowej w porównaniu do analiz numerycznych.

Received: 2024-04-20, Revised: 2024-05-28